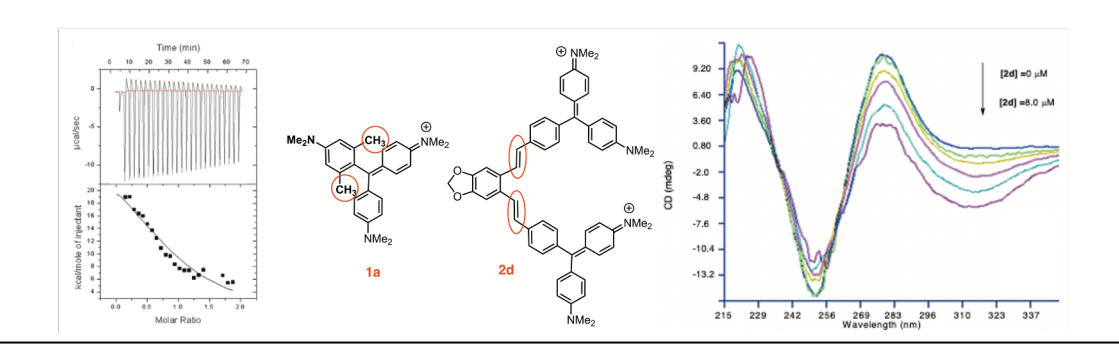
Graphical Abstract

DNA Major versus Minor Groove Occupancy of Monomeric and Dimeric Crystal Violet Derivatives. Toward Structural Correlations

Leave this area blank for abstract info.

Aren Mirzakhanian, Michael Khoury, Eli Trujillo, Byoula Kim, Donnie Ca, and Thomas G. Minehan*





Bioorganic & Medicinal Chemistry

journal homepage: www.elsevier.com

DNA Major versus Minor Groove Occupancy of Monomeric and Dimeric Crystal Violet Derivatives. Toward Structural Correlations

Aren Mirzakhanian, Michael Khoury, Eli Trujillo, Byoula Kim, Donnia Ca, and Thomas Minehan*

^aDepartment of Chemistry and Biochemistry, California State University, Northridge, 18111 Nordhoff Street, Northridge, CA 91330, USA

ARTICLE INFO

ABSTRACT

Article history:
Received
Received in revised form
Accepted
Available online

Keywords:
Triphenylmethane dyes
Nucleic acids
Major groove
Stereoelectronic interactions
Molecular docking

Six monomeric (1a-1f) and five dimeric (2a-2e) derivatives of the triphenylmethane dye crystal violet (CV) have been prepared. Evaluation of the binding of these compounds to CT DNA by competitive fluorescent intercalator displacement (FID) assays, viscosity experiments, and UV and CD spectroscopy suggest that monomeric derivative 1a and dimeric derivative 2d likely associate with the major groove of DNA, while dimeric derivatives 2a and 2e likely associate with the minor groove of DNA. Additional evidence for the groove occupancy assignments of these derivatives was obtained from ITC experiments and from differential inhibition of DNA cleavage by the major groove binding restriction enzyme BamHI, as revealed by agarose gel electrophoresis. The data indicate that major groove ligands may be optimally constructed from dye units containing a sterically bulky 3,5-dimethyl-N,N-dimethylaniline group; furthermore, the groove-selectivity of olefin-tethered dimer 2d suggests that stereoelectronic interactions ($n \rightarrow \pi^*$) between the ligand and DNA are also an important design consideration in the crafting of major-groove binding ligands.

1. Introduction

Major groove binding small molecules which can directly compete with transcription factors and other DNA binding proteins for their cognate sites on DNA have the potential to regulate gene expression. However, relatively few naturallyocurring substances associate with the major groove of DNA.2a The majority of nucleic acid-binding natural products prefer to occupy the narrower minor groove, where hydrophobic and van der Waals interactions with the walls and floor of the groove are maximized.2b Non-natural major groove binders have also been developed, such as ditercalinium,³ Iverson's naphthalene-diimide peptides,⁴ and Arya's neomycin-neomycin dimer⁵. More recently, Berdnikova demonstrated that mono- and bis-styryl dyes possessing an oxodecyl chain preferentially occupy the major groove of DNA.⁶ Furthermore, Mollica has shown that β-hairpin peptides and β-sheet analogs of the ARC protein bind the major groove with modest sequence selectivities.7 The cationic triphenylmethane dyes crystal violet (CV) and methyl green (MG) are histochemical stains known to bind duplex DNA by a nonintercalative mode of association.8 Evidence presented by Kim and Norden^{8d} suggests that methyl green binds the major groove of DNA. Motivated by these findings, we previously prepared dimeric and trimeric derivatives of crystal violet (CV) that displayed submicromolar affinities for duplex DNA; furthermore, competitive DNA binding studies and CD spectroscopy provided evidence that the tightest binding trimeric derivative most likely

associates with the major groove of DNA, with an approximately 10-fold preference for binding AT-rich homopolymers over GCrich sequences.⁹ It has been shown by Arya that sterically bulky major groove ligands prefer to bind the wider major groove of nonalternating AT-rich DNA (termed B*-form DNA)^{5b} over typical B-form DNA.⁵ To further probe ligand structural factors important for major versus minor groove binding, we designed a series of six monomeric CV derivatives (Figure 1) with varying degress of steric bulk, containing two (1a) or three (1b) methyl groups and one (1d), two (1e), or three (1f) phenyl groups on the aromatic rings of the dye, as well as an expanded dye possessing a naphthyl group (1c). In addition, five dimeric CV derivatives (Figure 2) were designed with dye units connected to an ortho-substituted aryl core by *ortho* or *para*-aryl (2a, 2b), alkynyl (2c), alkenyl (2d), or alkoxyalkyl (2e) linkers. The benzodioxole core employed for derivatives 2b, 2c, and 2d enhanced the stability of the dyes through resonance interaction of the oxygen lone pairs with the triphenylmethane carbocations, as also observed in dimer 2e; the less stable but more compact compound 2a with a phenyl core was prepared because of low yields encountered in the starting material synthesis with 5.6-dibromo-1.3-benzodioxole. We envisioned that the sp, sp², and sp³-hybridized linkers in compounds 2c, 2d, and 2e, respectively, would allow an assessment of the impact of extended charge delocalization from the peripheral dye units on ligand-DNA binding. The synthetic pathways to these

^{*} Corresponding author. Tel.: +1-818-677-3315; fax: +1-818-677-4068; e-mail: thomas.minehan@csun.edu

compounds, as well as analyses of their DNA binding mode and sequence selectivity, are detailed herein.

$$\begin{array}{c} \bigoplus_{\mathsf{NMe}(\mathsf{X})} \\ \bigoplus_{\mathsf{R}_2} \\ \mathsf{R}_3 \\ \mathsf{R}_4 \\ \mathsf{R}_1 \\ & \bigoplus_{\mathsf{NMe}_2} \\ \mathsf{Me}_2 \\ \mathsf{N}_{\mathsf{N}} \\ & \bigoplus_{\mathsf{NMe}_2} \\ \mathsf{NMe}_2 \\ & \bigoplus_{\mathsf{NMe}_2} \\ \mathsf{NMe}_2 \\ & \bigoplus_{\mathsf{NMe}_2} \\ \mathsf{NMe}_2 \\ & \bigoplus_{\mathsf{NMe}_2} \\ & \bigoplus_{\mathsf{NMe}_2} \\ \mathsf{NMe}_2 \\ & \bigoplus_{\mathsf{NMe}_2} \\ & \bigoplus_{\mathsf{NMe}_2} \\ & \bigoplus_{\mathsf{NMe}_2} \\ \mathsf{NMe}_2 \\ & \bigoplus_{\mathsf{NMe}_2} \\ & \bigoplus_{\mathsf{NMe}_2} \\ \mathsf{NMe}_2 \\ & \bigoplus_{\mathsf{NMe}_2} \\$$

Figure 1. Structures of the cationic dyes methyl green (MG), crystal violet (CV) and synthetic derivatives **1a-1f**.

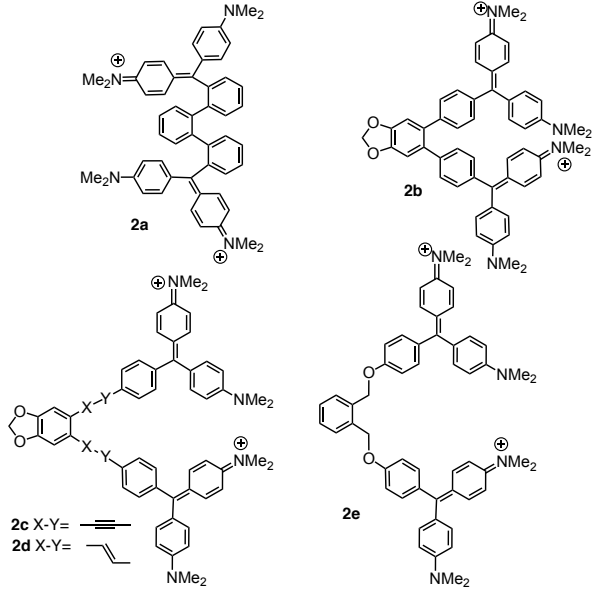


Figure 2. Structures of synthetic CV derivatives 2a-2e.

2. Results and Discussion

2.1 Chemistry

A slight modification of a reported protocol for the synthesis of triphenylmethane dyes¹⁰ was followed to prepare compounds 1a-1f. Three equivalents of 3-methyl-4-bromo-N,N-dimethylaniline was treated with n-BuLi (THF, -78 °C), and in 10 minutes ethyl-2-methyl-4-dimethylamino-benzoate was added; after stirring for 3 hours at room temperature, aqueous acidic workup and purification afforded compound 1b in 70% yield (Scheme 1). It was found that silica gel chromatography of the dye products resulted in very low (<20%) isolated yields, a problem that was ultimately circumvented by switching to size-exclusion chromatography using Sephadex LH-20. Reaction of 4-bromo-*N*,*N*dimethylaniline and ethyl-6-(dimethylamino)-2-naphthalenecarboxylate gave 1c in 57% yield. Further, compounds 1d, 1e, and 1f were prepared in 52%, 39%, and 65% yields, respectively, by an analogous reaction sequence from either 4-bromo-*N*,*N*-dimethylaniline or 2-phenyl-4-bromo-*N*,*N*dimethylaniline and either ethyl-4-dimethyl-aminobenzoate or ethyl-3-phenyl-4-dimethylaminobenzoate. Finally, ligand 1a was prepared in 75% isolated yield following the protocol of Barker, Bride, and Stamp¹¹ in which N,N-3,5tetramethylaniline was heated with Mischler's ketone in POCl₃ for 5 hours at 100 °C, followed by aqueous workup and purification.

For the preparation of dimeric CV derivatives, a protocol involving combination of excess aryllithium reagent with various

diesters was employed (see Supporting Information File). Thus, the reaction of five equiv of 4-lithio-*N*,*N*-dimethylaniline (obtained by treatment of 4-bromo-*N*,*N*-dimethylaniline with 1.1 equiv of *n*-BuLi in THF at -78 °C) with 1 equiv of diester, followed by warming to rt and aqueous acidic workup and purification, gave compounds **2a**, **2b**, **2c**, **2d** and **2e** in 43%, 63%, 53%, 40% and 61% yields, respectively (Scheme 2).

Scheme 1. Synthesis of ligands 1a-1f.

Scheme 2. Synthesis of ligands 2a-2e.

2.2 DNA binding evaluation

To evaluate the ability of these eleven compounds to recognize CT DNA, we performed competitive ethidium displacement assays12 in the presence and absence of the minor groove binder netropsin or the major groove binder methyl green, and compared C_{50} values (the concentration of ligand required to achieve a 50% decrease in the fluorescence of ethidium bromide, Figure 3 a,b) and apparent binding affinities (K_{app} =9.5x10⁶ M⁻¹ x C_{ethidium}/C₅₀, Table 1). The tightest binding monomeric CV derivative is 1e $(K_{app}=21.6\pm0.1 \text{ x } 10^6 \text{ M}^{-1})$ containing two phenyl groups attached to the triphenylmethane core. Comparing K_{app} values in the presence of netropsin or methyl green, it is apparent that compound **1a** $(K_{app}=9.5\pm0.4 \times 10^6 \,\mathrm{M}^{-1})$ provides the most compelling evidence for major groove occupancy, with a >8fold lower K_{app} value (1.1±0.1 x 10⁶ M⁻¹) recorded in the presence of methyl green, versus only a 1.3-fold lower value $(7.5\pm0.1 \text{ x } 10^6 \text{ M}^{-1})$ in the presence of netropsin. Further, compound **1d** $(K_{app}=1.63\pm0.02 \text{ x } 10^6 \text{ M}^{-1})$ displayed a 5-fold lower K_{app} value in the presence of methyl green (0.72±0.01

x 10^6 M⁻¹) versus in the presence of netropsin (3.54±0.16 x 10⁶ M⁻¹), an observation again suggestive of major groove occupancy. In contrast, compounds 1b, 1c, 1e, and 1f showed no strong preference for major or minor groove binding from competitive inhibition analysis. For CV derivatives 2a-2e, the tightest binding compound was 2a (K_{app} = 95±1.9 x 10⁶ M⁻¹), which together with derivative **2e** $(K_{app} = 33\pm 2.2 \times 10^6 \text{ M}^{-1})$ evidenced minor groove binding by displaying lower K_{app} values in the presence of netropsin (K_{app} = 62.5±2.4 x 10⁶ M⁻¹ and 9.5±0.2 x 10⁶ M⁻¹ for 2a and 2e, respectively) versus in the presence of methyl green (K_{app} =81.9±2.2 x 10⁶ M⁻¹ and 16.0±1.0 x 10⁶ M⁻¹ for 2a and 2e, respectively). Compound **2d** $(K_{app}=37.0\pm2.8 \text{ x } 10^6 \text{ M}^{-1})$ showed a strong preference for major groove binding, displaying a >8-fold lower apparent affinity for CT DNA in the presence of methyl green $(K_{app}=4.4\pm1.3 \text{ x } 10^6 \text{ M}^{-1})$ versus in the presence or absence of netropsin ($K_{app} \sim 37 \pm 3.0 \text{ x } 10^6 \text{ M}^{-1}$). Compound **2c** evidences a mixed binding mode, while compound 2b displays a preference for major groove binding. K values derived from ITC titrations of 1a-1f and 2a-2e with the DDD hairpin (Figure 8b) are provided for comparison in Table 1b.

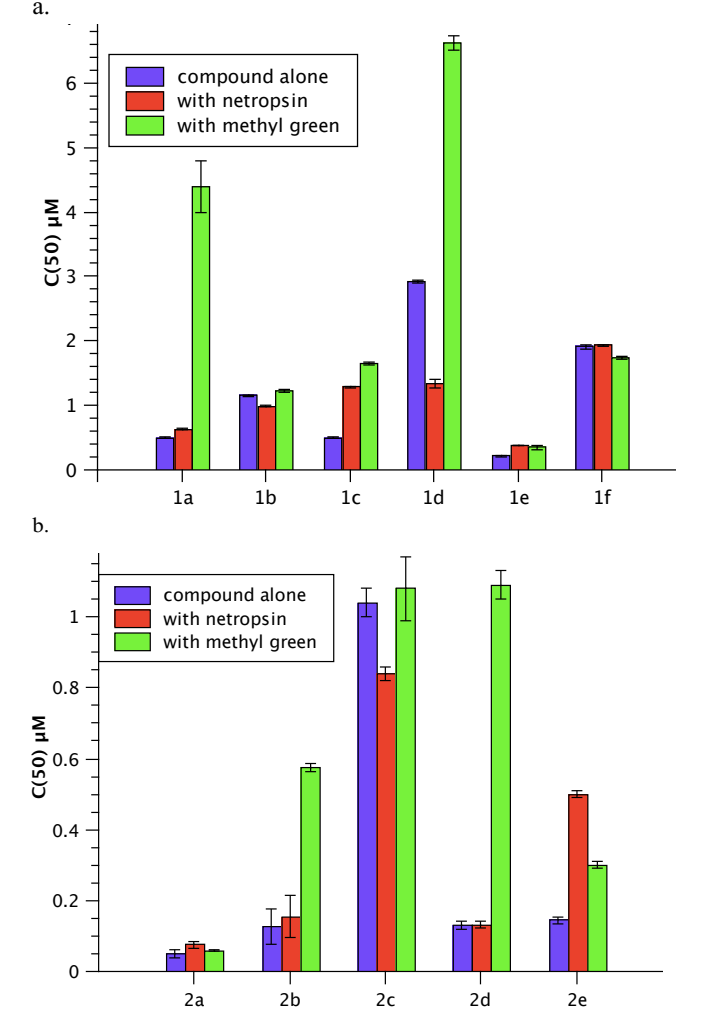


Figure 3. (a) C_{50} values (in μM) for the binding of compounds **1a-1f** to CT DNA (0.625 μM/bp, + 5 μM ethidium bromide, 10 mM Tris-HCl, pH=7.0) in the absence (blue bar) or presence of netropsin (2.0 μM, red bar) or methyl green (2 μM, green bar). (b) C_{50} values (in μM) for the binding of compounds **2a-2e** to CT DNA (1.0 μM/bp, + 0.5 μM ethidium bromide, 10 mM Tris-HCl, pH=7.0) in the absence (blue bar) or presence of netropsin (0.5 μM, red bar) or methyl green (0.5 μM, green bar). Error bars represent the standard deviation of three replicate experiments.

Table 1a. K_{app} , r_{bd} , and ΔT_M values for the binding of **1a-1f** and **2a-2e** to CT DNA in the presence or absence of netropsin or methyl green.

	K_{app}^{a}/K (x 10 ⁶ M ⁻¹)	r_{bd} b	<i>∆T_M</i> ^c (°C)	K_{app} + netropsin ^d (x 10 ⁶ M ⁻¹)	K_{app} + methyl green ^d (x 10 ⁶ M ⁻¹)
1a	9.5±0.4	2.2	2.8	7.5±0.1	1.1±0.1
1b	4.10±0.07	2.3	2.6	4.79±0.10	3.86±0.06
1c	9.5±0.2	3.1	4.6	3.68±0.03	2.87±0.06
1d	1.63±0.02	1.7	6.2	3.54±0.16	0.72±0.01
1e	21.6±0.1	4.2	1.6	12.5±0.3	13.6±0.1
1 f	2.48±0.04	4.3	2.2	2.46±0.01	2.10±0.03
2 a	95.0±1.9	3.0	3.6	62.5±2.4	81.9±2.2
2b	38±15	3.2	2.6	31±12	8.3±0.2
2c	4.6±0.2	3.5	2.6	5.7±0.1	4.4±0.4
2d	37.0±2.8	5.3	3.3	36.0±2.7	4.4±1.3
2 e	33.0±2.2	7.0	0.9	9.5±0.2	16.0±1.0

Table 1b. ITC-derived *K* values for the binding of **1a-1f** and **2a-2e** to the DDD hairpin (Figure 8b).^e

(1.56			
	K		K
	$(x 10^5 M^{-1})$		(x 10 ⁵ M ⁻¹)
1a	14.6±2.9	2 a	21.1±2.7
1b	1.2±0.5	2b	2.4±1.2
1c	3.1±0.6	2c	0.5±0.1
1d	96.4±4.5	2d	7.5±1.3
1e	0.3±0.1	2 e	20.5±9.5
1 f	48.7±1.3		

 a Average K_{app} values obtained by the ethidium displacement method $(K_{app}=K_e \times C_e/C_{50})$ bRatio of CT DNA(bp):ligand, as determined from the breakpoint of the curve in a plot of Δ Fluorescence vs. CT DNA:ligand ratio. ${}^5 \,{}^{\rm c} T_M$ values obtained from first derivative analysis ($\Delta A/\Delta T$ vs. ΔT) of the sigmoidal curves A_{260} vs. T; $\Delta T_M = T_M$ (CT DNA+ligand)- T_m (CT DNA); [CT DNA]=75 µM/bp; [ligand]=2.5 µM.27 d[netropsin] or [methyl green]=2.0 µM, [CT DNA]=0.625 µM/bp, and [ethidium bromide]=5 μM for 1a-1f; [netropsin] or [methyl green]=0.5 μM, [CT DNA]=1.0 μM/bp, and [ethidium bromide]=0.5 μM for 2a-2e. Initial addition of netropsin or MG to the CT DNA ethidium complex results in a 24.3±3.2% or 30.5±4.5% decrease, respectively, in ethidium fluorescence; the new fluorescence value after addition represents the initial fluorescence reading for titrations with compounds 1a-1f and 2a-2e. Red=likely minor groove binder; green=likely major groove binder. ^e K values (average of triplicate experiments) obtained from ITC titrations of DDD hairpin (10 µM) with ligand (100 µM in syringe).

Monitoring the titrations of compounds 1a, 2a, 2d, and 2e with CT DNA by UV spectroscopy²⁹ revealed hypochromic and bathochromic shifts in the main dye absorption bands centered around 375-450 nm and 600-620 nm (see Figure 4a and Supporting Information file). Such shifts have been observed for both intercalating and groove binding compounds.¹³ To verify that the dye derivatives are groove binders and not intercalators, we performed CT DNA solution viscosity experiments with compounds 1a, 2a, 2d and 2e. The lengthening and rigidification of DNA that results from intercalation of drugs between the base-pair stack has been shown to give rise to an increase in solution viscosity.¹⁴ Figure 4b shows a plot of the relative viscosities of intercalator control compound ethidium bromide and 1a versus the ligand/DNA ratio. Whereas increasing concentrations of ethidium bromide increases the viscosity of the CT DNA solution, increasing concentrations of 1a show minimal changes in CT DNA solution viscosity over the concentration range studied. Similar results were obtained for compound 2a as well as control compound methyl green. However, increasing concentrations of the larger dyes 2d and **2e** showed a slight *decrease* in CT DNA solution viscosity. A decrease in solution viscosity may result from a groove binding mode that induces DNA bending. 32

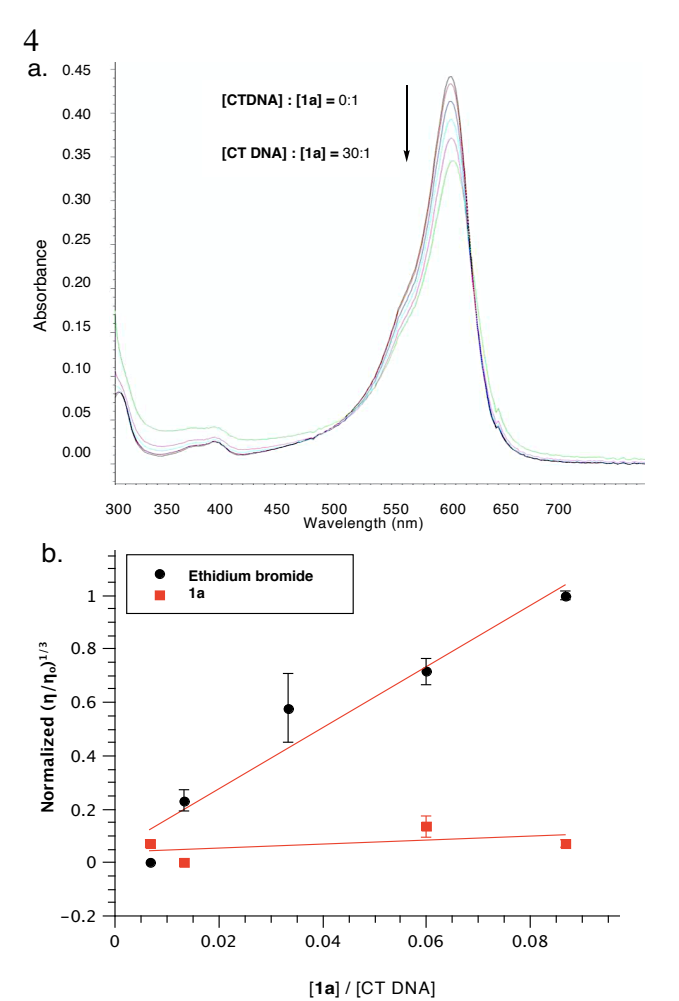


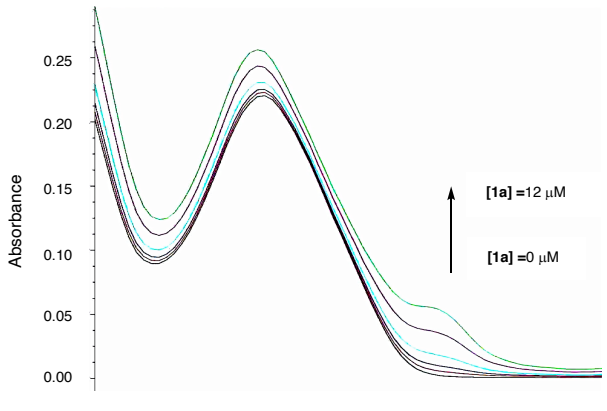
Figure 4. a. UV titration of **1a** in 10 mM Tris-HCl buffer, pH = 7.0: [**1a**] = 5.0 μM; [CT DNA] : [**1a**] = 0:1 (black line); 1:1 (red line); 2:1 (blue line); 5:1 (teal line); 10:1 (purple line); 30:1 (green line). b. Solution viscosity studies for **1a** in 10 mM Tris-HCl, pH=7.0: [CT DNA] = 300 μM/bp; [ethidium]= 0.0, 2.0, 4.0, 10.0, 18.0, 26.0 μΜ; [**1a**] = 0.0, 2.0, 4.0, 10.0, 18.0, 26.0 μΜ. Error bars represent the standard deviation of three replicate experiments

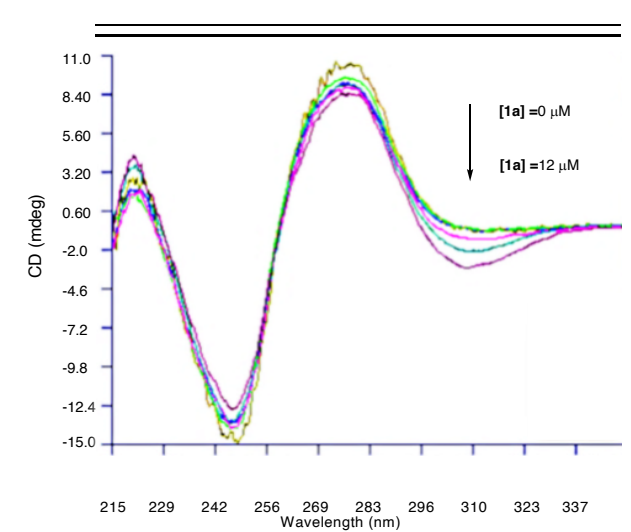
Data from circular dichroism experiments provided additional support for the groove occupancy assignments of 1a, 1d, 2a, 2d, and 2e. Wilson et al. 15a have reported that titrations of DNA with groove binders produce positive induced CD (ICD) bands, while Garoufis^{15b} and Hannon^{15c} have indicated the development of negative ICD bands. To establish a reference point for our system, we observed that titration of CT DNA with the structurally similar major groove binding dye methyl green results in a strong negative induced CD band (ICD) at 310 nm (see Supporting Information file). Repetition of the CD experiments with a DNA hairpin containing the Drew-Dickerson dodecamer (DDD) sequence (Figure 8b)²⁵ yielded very similar results to those obtained with CT DNA. As can be seen in Figures 5a and 5b, CD titrations of the DDD hairpin with compounds 1a and 2d both produce negative ICD bands at ~310 nm (a similar profile was observed for titration of CT DNA with 1d), corresponding to the UV absorption of the bound dye at the same wavelength.¹⁵ Furthermore, although titrations of 2d with the DDD oligo show a strong decrease in the base stacking band (280 nm) at higher 2d:DNA ratios, negligible changes in the helicity band at 245 nm are observed over the same concentration range, an observation inconsistent with intercalative binding.16a

In contrast, CD spectra of titrations of CT DNA with **2a** and **2e** showed positive ICD bands above 300 nm (Figure 5 c,f). ^{16b} The bisignate nature of the 335 nm ICD band of **2e** may be indicative of dye aggregation in the DNA groove; ⁶ in addition, two new absorptions at 310 and 337 nm observed in

UV spectral titrations of **2e** with CT DNA, attributable to the bound (DNA-dye) complex, lend support to this hypothesis.

Compound 1a





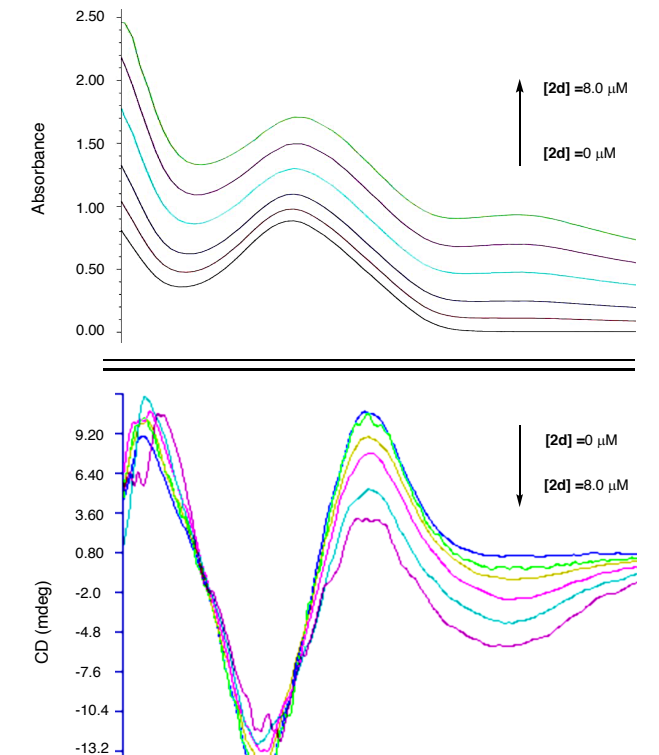
b. Compound 2d

215

229

256

269 283 Wavelength (nm)

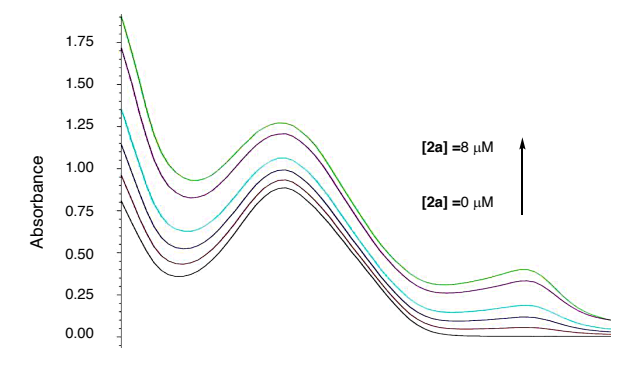


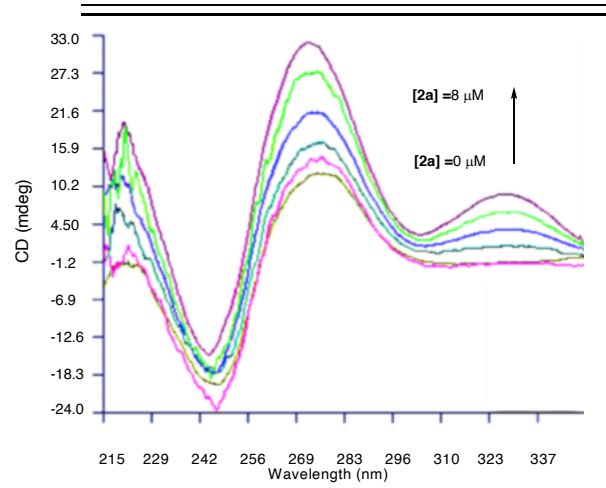
310

323 337

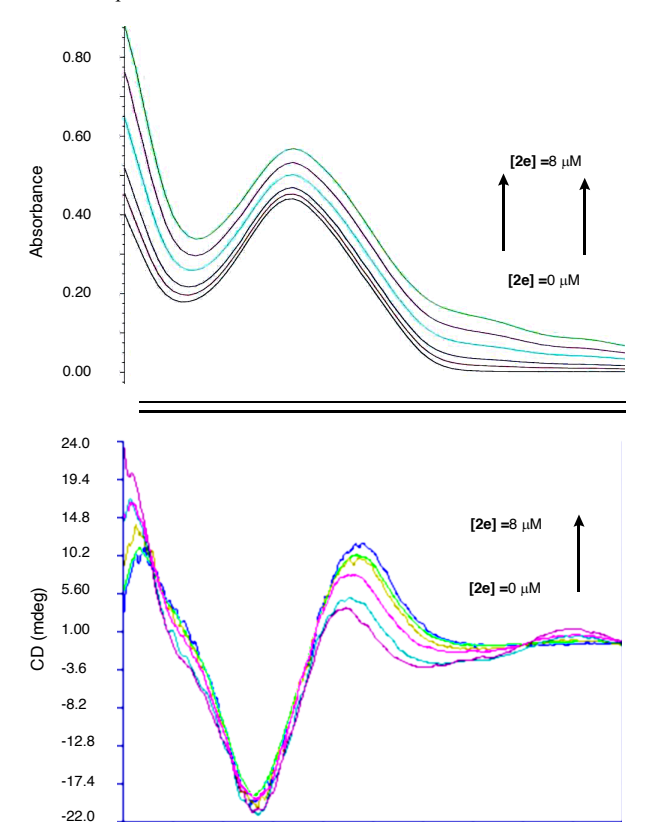
296

c. Compound 2a:





d. Compound 2e:



56 269 283 Wavelength (nm)

Figure 5. a. The 220–350 nm region of the UV and CD spectra of solutions of DDD hairpin (8.8 μM, 10 mM Tris-HCl, pH=5.0) in the presence of various concentrations of a. **1a**: 0.0 μM, 0.9 μM, 2.0 μM, 4.0 μM, 8.0 μ, and 12.0 μM; b. **2d**: 0.0 μM, 0.9 μM, 2.0 μM, 4.0 μM, 6.0 μM, and 8.0 μM; c. **2a**: 0.0 μM, 0.9 μM, 2.0 μM, 4.0 μM, 6.0 μM, and 8.0 μM; d. **2e**: 0.0 μM, 0.9 μM, 2.0 μM, 4.0 μM, and 8.0 μM.

ITC titrations¹⁷ of CT DNA (100 μ M/bp) with compounds 1a, 2d, and 2e (100 μ M solutions, 25 °C, pH=7.0, 10 mM Tris-HCl buffer) provided thermodynamic data also suggestive of differential groove occupancy.^{17e} Whereas the binding of compound 2e is clearly enthalpy driven (Δ H=-44.7 kcal/mol, Δ S=-120 cal/mol•K, Figure 6), the data for both 1a and 2d clearly indicate an entropy-driven process (Δ H=29.7 kcal/mol, Δ S=122 cal/mol•K for 1a, Figure 6; Δ H=85.8 kcal/mol, Δ S=316 cal/mol•K for 2d). A strong entropic contribution to the binding free energy is characteristic of agents that associate with the major groove of DNA due to the release of bound water molecules to bulk solvent upon binding.¹⁸

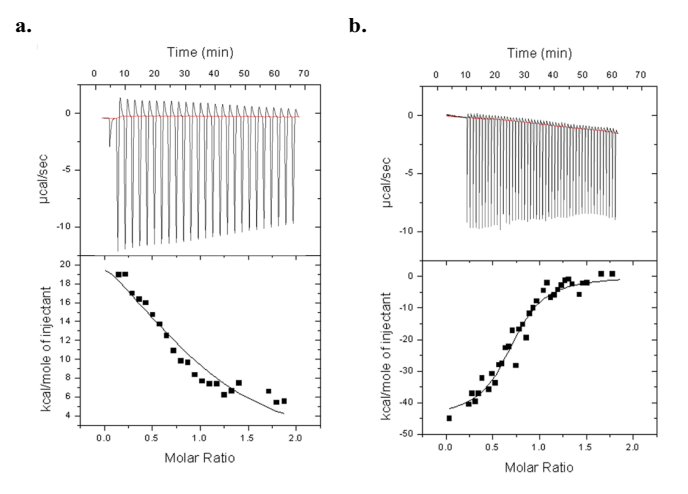


Figure 6. ITC thermograms for the binding of **1a** (a) and **2e** (b) to CT DNA (100 μM/bp, 10 mM Tris-HCl, pH=7.0). **1a**: N=1.0, K=1.9±0.5x10⁵M⁻¹, Δ H=29.8±2.5 kcal/mol, Δ S=122 cal/mol•K; **2e**: N=0.73, K=2.1±0.5x10⁶ M⁻¹, Δ H=-44.7±2.2 kcal/mol, Δ S=-120 cal/mol•K.

To obtain additional support for the DNA binding mode of the synthetic CV derivatives, we examined cleavage of pUC-19 plasmid DNA by the major-groove binding restriction enzyme BamH1 (5'-G^GATCC-3')¹⁹ in the presence of the major and minor-groove binding small molecules methyl green and netropsin, respectively.³⁰ Whereas the concentration of methyl green required to achieve 50% inhibition of DNA cleavage (IC₅₀) by BamH1 was 77 μ M, the concentration of netropsin required to achieve the same level of cleavage inhibition was greater than 600 μ M.²⁰ In the same manner, whereas the IC₅₀ for the putative major groove binder **2d** was 5.4 μ M, the IC₅₀ for the putative minor groove binder **2a** was 67 μ M. Thus, an approximately order of magnitude difference or greater in IC₅₀ values was observed for major vs. minor groove binders in plasmid cleavage by BamH1 (Figure 7).

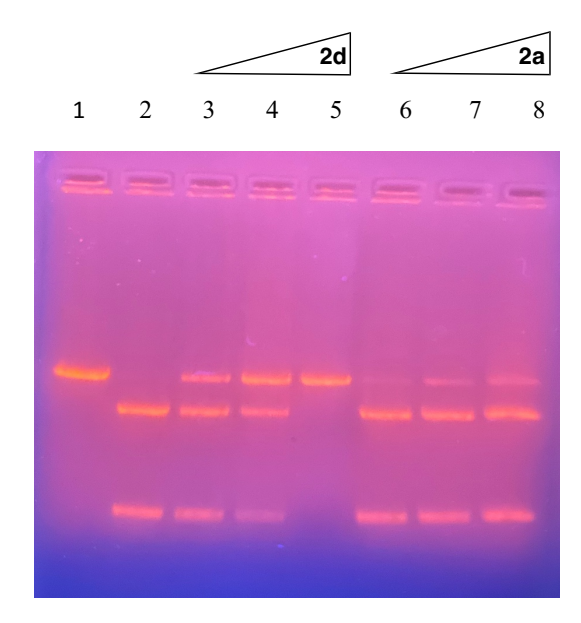


Figure 7. Cleavage of plasmid pUC-19 (linearized with AlwN1, lane 1) by Bam H1 in the presence of **2d** (lanes 3-5) or **2a** (lanes 6-8). Ligand concentrations: lane 2: 0 μ M; lane 3: 3 μ M **2d**; lane 4: 6 μ M **2d**; lane 5: 25 μ M **2d**; lane 6: 3 μ M **2a**; lane 7: 6 μ M **2a**; lane 8: 25 μ M **2a**. IC₅₀ (**2d**) =5.4 μ M; IC₅₀ (**2a**) =67 μ M.

Finally, we examined the sequence selectivity of our synthetic crystal violet derivatives by performing fluorescent intercalator displacement (FID) experiments with a series of oligonucleotides.²¹ Three separate hexadecamers, A₅T₅ (5'-GGGAAAAATTTTTCCCCC-3'), (AT)5 (5'-GGGATATA-TATATCCC-3') ((AT)5) and G₅C₅ (5'-AAAGGGGG-CCCCCTTT-3') (all at 10 µM/bp) were titrated with compounds 1a-1f in the presence of ethidium bromide (5 μM). The percent ethidium displacement at 2 μM of each ligand was recorded (see Supporting Information file), as well as the C_{50} value (Table 2a). As can be seen from the data shown, monomeric CV derivatives showed little sequence discrimination, with only the sterically bulky compound 1b showing a slight (>3-fold) preference for AT-rich DNA (C_{50} =~2.4 μ M for A_5T_5 and $(AT)_5$) over GC rich DNA $(C_{50}=7.2 \mu M \text{ for G5C5}).$

For the dimeric compounds (Figure 8a and Table 2b), FID assays were used to assess the sequence selectivity of 2a-2e for hairpin oligonucleotides (Figure 8b) containing consensus sequences for the cancer-relevant transcription factors NFAT1 (5-GAAAAA-3'),²² STAT6 (5'-TCCTAG-3'),²³ cMyc (5'-CACGTG-3'),24 as well as the Drew-Dickerson sequence (5'-GAATTC-3'),25 5'-ATATAT-3', and 5'-GGGGG-3'. Once again, low sequence discrimination was observed, with major-groove binding compound 2d showing a slight (1.4-fold) preference for binding the AT-rich Drew-Dickerson sequence over the other oligonucleotoides, and minor groove binding compound 2e showing a modest preference for binding GC-rich sequences over AT-rich sequences. ITC titrations of 1a, 2a, 2d, and 2e with the six hairpins (Table 2c) also revealed the moderate ~6-fold preference of compound 2d for the AT-rich sequence of NFAT1 over the other oligonucleotides, as well as the preference of 2e for the GC rich sequences found in the cMyc and GC hairpins.

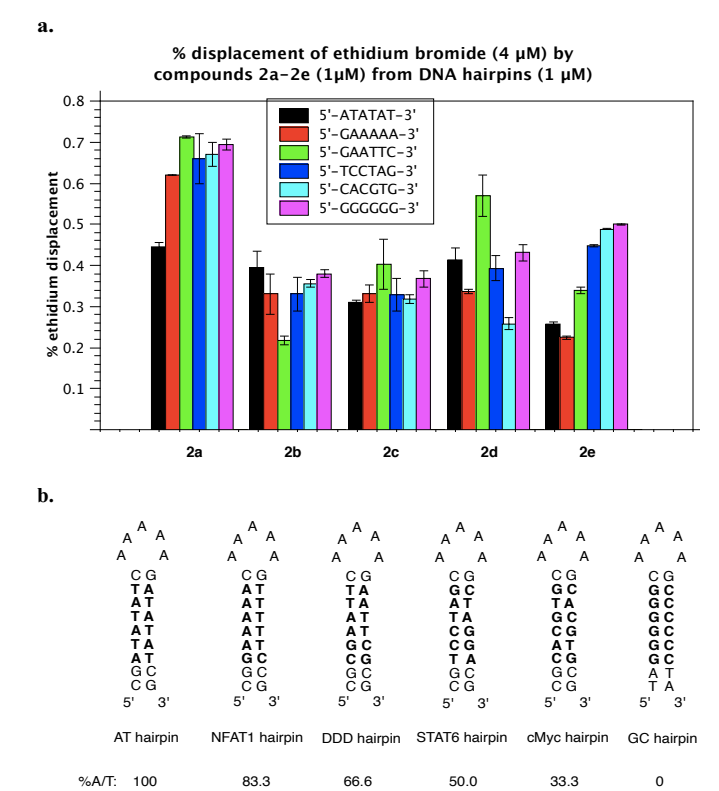


Figure 8. a. Chart showing the percent displacement of ethidium bromide $(4 \mu M)$ from hairpin oligonucleotides 5'-ATATAT-3', 5'-GAAAAA-3', 5'-TCCTAG-3', 5'-CACGTG-3', 5'-GAATTC-3', and 5'-GGGGGG-3' (all at 1 μM) by **2a-2e** $(1 \mu M)$. b. Structure of hairpin oligonucleotides employed. Experiments performed in 10 mM Tris-HCl buffer, pH=7.0.

employ a.	yed. Experii	nents perfo	rmed in 10	0 mM Tris-I	HCI buffer,	pH=7.0.	
		A ₅ T ₅		(AT) ₅	G	G₅C₅	
		(μM)		(μM)	(μM)		
	1a	1.86±0.	1.86±0.01		2.05±0.11		
	1b	2.40±0.	2.40±0.02		7.21±0.63		
	1c		0.52±0.01		0.88±0.01		
	1d	2.61±0.	2.61±0.02		2.99±0.01		
	1e	1.83±0.01		1.81±0.01	2.09±0.06		
	1f	3.13±0.01		2.71±0.03	3.36±0.07		
b.							
	(AT)₃	NFAT1	DDD	STAT6	сМус	G_6	
	(μM)	(μM)	(μM)	(μM)	(μM)	(μM)	
2a	1.11	0.69	0.54	0.56	0.57	0.51	
	±0.03	±0.03	±0.02	±0.01	±0.03	±0.11	
2b	1.36	1.23	1.47	1.32	1.42	1.25	
	+0.04	±0.08	±0.03	±0.20	±0.05	±0.16	
2c	1.52	2.22	1.27	1.91	1.95	1.32	
	±0.02	±0.13	±0.34	±0.25	±0.15	±0.12	
2d	1.21	1.27	0.78	1.12	1.80	1.10	
	±0.07	±0.05	±0.08	±0.04	±0.06	±0.04	
2e	2.08	2.64	1.57	1.09	1.56	1.00	
	±0.01	±0.05	±0.02	±0.02	±0.01	±0.03	
c.							
	(AT)₃	NFAT1	DDD	STAT6	сМус	G_6	
	K	Κ	Κ	Κ	K	K	
	(x10 ⁵ M ⁻¹)						
1a	0.21	0.19	14.6	1.06	12.6	28.3	
	±0.07	±0.04	±2.9	±0.63	±3.4	±6.7	
2a	0.32	1.14	21.1	1.80	1.14	52.8	
	±0.08	±0.32	±2.7	±0.66	±0.29	±22.7	
2d	5.79	49.8	7.54	2.22	0.32	0.18	
	±4.29	±10.3	±1.26	±0.42	±0.15	±0.09	
2e	1.3	29.1	20.5	1.32	50.6	36.5	
	±0.38	±9.2	±9.6	±0.57	±7.65	±14.4	
Table	2. a. C ₅₀ dat	a for the bi	nding of 1	a-1f to A ₅ T	, (AT) ₅ , and	d G ₅ C ₅ . b.	
C 1-	4 - C 41 1	. :	2- 2- 4-	1		(AT)	

Table 2. a. C_{50} data for the binding of **1a-1f** to A_5T_5 , $(AT)_5$, and G_5C_5 . b. C_{50} data for the binding of **2a-2e** to hairpin oligonucleotides $(AT)_3$, NFAT1, STAT6, cMyc, Drew-Dickerson, and G_6 . c. ITC-derived K values (average of triplicate experiments) for the binding of **1a**, **2a**, **2d**, and **2e** (100 μ M in syringe) to DNA hairpins oligonucleotides (10 μ M).

2.3 Molecular docking studies

Concerning structural factors that may favor major vs. minor groove binding, ligand docking studies (using AutoDock vina²⁶) with the Drew-Dickerson dodecamer (PDB 436D)²⁵ revealed that whereas compound **1a** localized in the major groove (Figure 9a), compound 1b, with similar steric bulk, preferred docking in the minor groove. It is noted that the 3,5-dimethyl substitution of **1a** renders a near orthogonal arrangement of the aryl ring planes in this compound, resulting in a ligand span that achieves close electrostatic contact between the electropositive dimethylamino group and the phosphate groups on opposite sides of the major groove. For 2d, molecular docking with the NFAT sequence (PDB 1OWR)²² indicates that the trans olefin tether is oriented in proximity to the nitrogen and oxygen atoms of the adenine and guanine bases in the major groove (Figure 9b). As can be seen from the electrostatic potential maps of 2d and the major groove base pairs of 5'-GA-3' (Figure 9c),31 the electrophilic character of the dye units is transmitted to the olefin tethers through the connecting π network, possibly allowing a favourable interaction with the O, N lone pairs $(n \rightarrow \pi^*)^{27}$ on the edges of the bases in the major groove. For dimer 2e with the saturated alkoxyalkyl tether, no such interaction with the linker is possible, and the flexible ligand can obtain more favourable hydrophobic interactions in the minor groove. As a result, the high electronegative potential of the major groove^{5b,28} appears to favour the binding of ligands that delocalize positive charge from the dye moieties onto the connecting linkers.

3. Conclusions

In summary, we have prepared a series of monomeric and dimeric derivatives of the histochemical stain crystal violet and investigated their DNA binding mode by CD spectroscopy, ITC, viscosity studies, fluorescence spectroscopy, and agarose gel electrophoresis. In the monomeric series, the derivative that displays the strongest preference for major groove occupancy is compound 1a, possessing the sterically bulky 3,5-dimethylaniline group; the perpendicular arrangement of the aryl rings enforced by this substitution allows the ligand to neatly span the major groove with likely one ionic contact with the phosphate backbone. In the dimeric series, compound 2d, possessing olefin linkers between the *ortho*-substituted aromatic core and the peripheral dye units, displays the strongest preference for major groove occupancy. Comparing the data obtained for the binding of 2d and 2e to DNA, the olefin linkers likely favor major groove binding through charge delocalization from the positively charged dyes to the central region of the molecule, allowing stereoelectronic interactions between the alkene π^* orbitals and the N, O lone pair (n) orbitals of the G and A bases. This study highlights the fact that a subtle balance between steric, hydrophobic, and stereoelectronic interactions determines the DNA groove localization of crystal violet derivatives.

Given the generally higher affinities of the dimeric series derivatives, future ligand optimization will be focused on designing dyes that have a combination of steric bulk at the dye termini (in the form of 3,5-dimethylaniline-type substitution), and linker functionality that allow favorable stereoelectronic interactions with the edges of the bases on the floor of the major groove. For the long-term goal of designing sequence specific DNA-binding small molecules capable of interfering with protein binding and gene expression *in vitro* and *in vivo*, future CV derivatives will need to incorporate additional functionality capable of distinguishing sequence context at their major groove

binding sites. Alternatively, since it is known that major groove width varies as a function of the DNA sequence,⁵ it may be possible to utilize appropriately designed sterically bulky CV derivatives as shape-selective DNA binding molecules.

4. Experimental part

4.1 General

Distilled water was used in all of the experiments. Reagents and solvents were used as supplied, with the following exceptions: CH₂Cl₂ was distilled from CaH₂; Et₂O was distilled from LiAlH₄; THF was distilled from sodium benzophenone ketyl; toluene and benzene were dried over 4Å molecular sieves. Organic extracts were dried over Na₂SO₄, filtered, and concentrated using a rotary evaporator at aspirator pressure (20-30 mmHg). Chromatography refers to flash chromatography and was carried out on SiO₂ (silica gel 60, 230-400 mesh). ¹H and ¹³C NMR spectra were measured in CDCl₃ at 400 MHz and 100 MHz, respectively, using Me₄Si as internal standard. Chemical shifts are reported in parts per million (ppm) downfield (δ) from Me₄Si. For ¹H NMR, multiplicity (s=singlet, d=doublet, dd=doublet of doublets, t=triplet, q=quartet, br=broad, m=multiplet) and coupling constants (in Hz) were reported whenever possible. 13C spectra were recorded with complete proton decoupling.

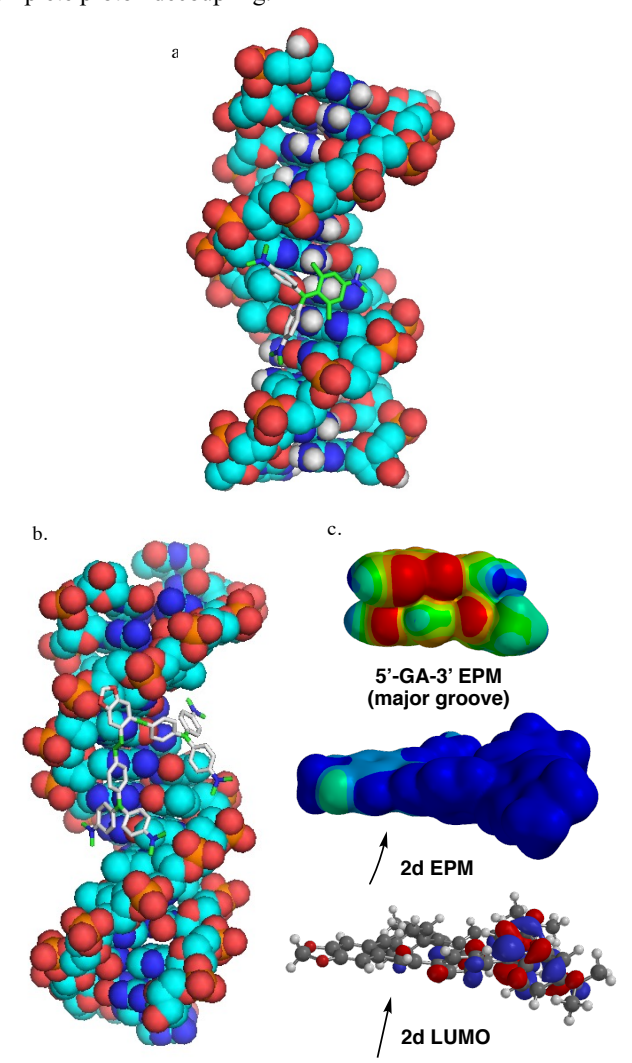


Figure 9. a. Model for the binding of ligand **1a** in the major groove of Drew Dickerson dodecamer DNA (5'-CGCGAATTCGCG-3'). b. Model for the binding of ligand **2d** in the major groove of the NFAT1 sequence (5'-GGAAAAA-3'). c. Electrostatic potential maps for the major groove base pairs of 5'-GA-3' and **2d**, and LUMO map of **2d**. Arrow points to the alkene moiety.

4.1.1 Synthesis of 1a

Following a known procedure, 11 3,5-dimethyl-N,N-dimethylaniline (1g, 6.7 mmol) was combined with Mischler's ketone (1.87 g, 7 mmol) in POCl₃ (1.1g, 7 mmol) and the mixture was heated in a sealed tube at 100 °C for 8 hours. Upon cooling to room temperature, the mixture was treated with a saturated aqueous solution of K₂CO₃ (20 mL) and ethyl acetate (20 mL), and the phases were separated. The aqueous phase was extracted with ethyl acetate (2 x 20 mL) and the combined organic phases were dried over anhydrous Na₂SO₄, filtered and concentrated in vacuo. The crude material was taken up in EtOAc (20 mL) and extracted with 1M HCl (3x 20 mL), and the layers were separated. The aqueous phase was further extracted with ethyl acetate (2 x 20 mL) and the combined organic phases were dried over anhydrous Na₂SO₄, filtered and concentrated in vacuo. Purification of the residue by size-exclusion chromatography (Sephadex LH-20, chloroform) afforded 1a (2.2 g, 5.0 mmol, 75%) as a dark blue solid, m.p. 223-226 °C (dec.). ¹**H NMR** (400 MHz, CDCl₃) δ 7.31 (m, 4H, Ar-H_{metaNMe2}); 7.25 (m, 2H, Ar-H_{orthoNMe2}); 6.98 (m, 4H, Ar-H_{orthoNMe2}); 3.32 (s, 12H, Ar-N(CH₃)₂); 3.21 (s, 6H, Ar- $N(CH_3)_2$); 1.87 (s, 6H, Ar-C H_3). ¹³C NMR (100 MHz, CDCl₃) δ 156.8 (C=NMe₂), 140.5 (C-Ar₃), 139.1 (C-CH₃), 127.4 (Cmeta,paraCNMe2), 114.2 (CorthoCNMe2), 41.2 (Ar-N(CH3)2), 21.0 (Ar-CH₃). **HRMS-ESI** (m/z): calculated for C₂₇H₃₄N₃ 400.2747 (M⁺), found 400.2741 (M⁺). UV (10 mM Tris-HCl, 0.1M NaCl, pH=7.06): λ_{max} 208 nm (ϵ 29758), 256 (8197), 306 (16925), 396 (9300), 614 (118847).

4.1.2 Synthesis of 1b

3-methyl-4-bromo-*N*,*N*-dimethylaniline (1 g, 4.69 mmol) was dissolved in THF (10 mL) and cooled to -78 °C. n-BuLi (2.1 mL, 2.3M in cyclohexane, 4.8 mmol) was added dropwise and the solution was stirred at -78 °C for 15 minutes. Then ethyl-2-methyl-4-dimethylaminobenzoate (345 mg, 1.66 mmol) dissolved in THF (2 mL) was added dropwise at -78 °C. The solution was allowed to warm to room temperature and stir overnight. A solution of 1M HCl (10 mL) was then added and the mixture was stirred for 30 minutes. Ethyl acetate (20 mL) was added and the phases were separated. The aqueous phase was further extracted with ethyl acetate (3x 10 mL); the combined organic extracts were once washed with 20 ml sat. aq. NaCl, dried over anhydrous Na₂SO₄, filtered, and concentrated under reduced pressure. Purification of the residue by size-exclusion chromatography (Sephadex LH-20, Chloroform) afforded **1b** (521 mg, 1.12 mmol, 70%) as a blue oil. ¹**H NMR** (400 MHz, CDCl₃) δ 6.95 (d, *J*=9.6 Hz, 3H, Ar- $H_{metaNMe2}$); 6.65 (m, 6H, Ar- $H_{orthoNMe2}$); 3.26, (s, 18H, Ar-N(C H_3)₂); 1.89 (2, 9H, Ar-CH₃). ¹³C NMR (100 MHz, CDCl₃) δ 155.1 (C-NMe2), 140.1 (C_{paraCNMe2}), 131.2 (C-CH₃, C-Ar₃), 115.7 (C_{orthoCNMe2}), 110.4 (C_{orthoCNMe2}), 40.5 (Ar-N(CH₃)₂), 22.2 (Ar-CH-3). **HRMS-ESI** (m/z): calculated for $C_{28}H_{36}N_3$: 414.2904 (M⁺), found 414.2895 (M⁺). UV (10 mM Tris-HCl, 0.1M NaCl, pH=7.06): λ_{max} 210 nm (ϵ 70957), 256 (34425), 308 (32063), 372 (14442), 618 (122188).

4.1.3 Synthesis of 1c

4-bromo-*N*,*N*-dimethylaniline (1 g, 5 mmol) was dissolved in THF (10 mL) and cooled to -78 °C. *n*-BuLi (2.17 mL, 2.3 M in cyclohexane, 5 mmol) was added dropwise and the solution was stirred at -78 °C for 15 minutes. Then ethyl-6-dimethylamino-2-napthalenecarboxylate (404 mg, 1.66 mmol) dissolved in THF (2 mL) was added dropwise at -78 °C. The solution was allowed to warm to room temperature and stir overnight. A solution of 1M HCl (10 mL) was then added and the mixture was stirred for 30 minutes. Ethyl acetate (20 mL) was added and the phases were

separated. The aqueous phase was further extracted with ethyl acetate (3x 10 mL); the combined organic extracts were once washed with 20 ml sat. aq. NaCl, dried over anhydrous Na₂SO₄, filtered, and concentrated under reduced pressure. Purification of the residue by size-exclusion chromatography (Sephadex LH-20) afforded 1c (343 mg, 0.95 mmol, 57%) as a dark green solid, m.p. 197-200°C (dec). ¹H NMR (400 MHz, CDCl₃): δ 7.65 (d, *J*=8.7 Hz, 1H, Ar-*H*); 7.60 (m, 2H, Ar-*H*); 7.38 (d, *J*=8.8 Hz, 4H, Ar-*H*); 7.19-7.16 (dd, *J*=2.5, 9.2 Hz, 2H, Ar-*H*); 6.91 (d, *J*=9.3 Hz, 5H, Ar-H); 3.32 (s, 12H, Ar-N(C H_3)₂); 3.18 (s, 6H, Ar-N(C H_3)₂). ¹³C **NMR** (100 MHz, CDCl₃): δ 178.8 (*C*-Ar₃), 156.2 (*C*=NMe₂), 151.5 (CNMe₂), 140.6 (C_{Ar}), 139.2 (C_{Ar}), 138.5 (C_{Ar}), 132.2 (C_{Ar}), 131.7 (C_{Ar}), 127.3 (C_{Ar}), 126.2 (C_{Ar}), 125.3 (C_{Ar}), 116.6 ($C_{orthoCN}$ Me2), 113.1 (CorthoCNMe2), 104.8 (CorthoCNMe2), 40.9 (Ar-N(CH₃)₂), 40.4 (Ar-N(CH_3)₂). **HRMS-ESI** (m/z): calculated for C₂₉H₃₂N₃ 422.2591 (M⁺), found 422.2559 (M⁺). UV (10 mM Tris-HCl, 0.1M NaCl, pH=7.06): λ_{max} 256 nm (ϵ 42045), 306 (37445), 614 (42815).

4.1.4 Synthesis of 1d

4-bromo-N,N-dimethylaniline (1 g, 5 mmol) was dissolved in THF (10 mL) and cooled to -78 °C. n-BuLi (2.17 mL, 2.3M in cyclohexane, 5 mmol) was added dropwise and the solution was stirred at -78 °C for 15 minutes. Then ethyl-3-phenyl-4dimethylaminobenzoate (447 mg, 1.66 mmol) dissolved in THF (2 mL) was added dropwise at -78 °C. The solution was allowed to warm to room temperature and stir for four hours. A solution of 1 M HCl (10 mL) was then added and the mixture was stirred for 30 minutes. Chloroform (20 mL) was added and the phases were separated. The aqueous phase was further extracted with chloroform (3x 10 mL); the combined organic extracts were once washed with 20 ml sat. aq. NaCl, dried over anhydrous Na₂SO₄, filtered, and concentrated under reduced pressure. Purification of the residue by size exclusion chromatography (Sephadex LH-20) afforded 1d (420 mg, 0.87 mmol, 52%) as a dark blue solid, m.p. 153-155 °C. ¹H NMR (400 MHz, CDCl₃) δ 7.38-7.36 (m, 7H, Ar-H); 7.32 (dd, J=6.4, 8.7 Hz, 2H, Ar-H); 7.28 (s, 1H, Ar-H); 7.18 (s, 1H, Ar-H_{orthoPh}); 7.11 (d, J=8.8 Hz, 1H, Ar-H_{orthoNMe2}); 6.91 (d, J=9.3 Hz, 4H, Ar-H_{orthoNMe2}); 3.31 (s, 12H, Ar-N(CH₃)₂); 2.87 (s, 6H, Ar-N(CH₃)₂). ¹³C NMR (100 MHz, CDCl₃) δ 177.7 (C-Ar₃), 156.6 (C=NMe₂), 155.9 (C-NMe₂), 141.8 (C_{Ar}), 140.8 (C_{Ar}), 140.1 (C_{Ar}) , 137.6 (C_{Ar}) , 130.5 (C_{Ar}) , 129.2 (C_{Ar}) , 128.8 (C_{Ar}) , 128.1 (C_{Ar}), 127.3 (C_{Ar}), 126.9 (C_{Ar}), 116.8 (C_{orthoCNMe2}), 112.7 (CorthoCNMe2), 43.2 (Ar-N(CH3)2), 40.8 (Ar-N(CH3)2). HRMS-ESI (m/z): calculated for $C_{31}H_{34}N_3$ 448.2747 (M⁺), found 448.2771 (M⁺). UV (10 mM Tris-HCl, 0.1M NaCl, pH=7.06): λ_{max} 210 nm $(\varepsilon 46240)$, 308 (17193), 600 (85290).

4.1.5 Synthesis of 1e

2-phenyl-4-bromo-*N*,*N*-dimethylaniline (1 g, 3.63 mmol) was dissolved in THF (10 mL) and cooled to -78 °C. *n*-BuLi (1.65 mL, 2.3 M in cyclohexane, 3.8 mmol) was added dropwise and the solution was stirred at -78 °C for 15 minutes. Then ethyl-4-dimethylaminobenzoate (233 mg, 1.21 mmol) dissolved in THF (2 mL) was added dropwise at -78 °C. The solution was allowed to warm to room temperature and stir for 4 hours. A solution of 1M HCl (10 mL) was then added and the mixture was stirred for 30 minutes. Chloroform (20 mL) was added and the phases were separated. The aqueous phase was further extracted with chloroform (3x 10 mL); the combined organic extracts were once washed with 20 ml sat. aq. NaCl, dried over anhydrous Na₂SO₄, filtered, and concentrated under reduced pressure. Purification of

the residue by size exclusion chromatography (Sephadex LH-20) afforded **1e** (264 mg, 0.47 mmol, 39%) as a dark blue solid, m.p. 116-118 °C (dec). **¹H NMR** (400 MHz, CDCl₃) δ 7.41–7.34 (m, 14H, Ar-H); 7.26-7.25 (d, J=2.2 Hz, 2H, Ar- $H_{orthoPh}$); 7.17 (d, J=8.9 Hz, 2H, Ar- $H_{orthoNMe2}$); 6.99 (d, J=9.2 Hz, 2H, Ar- $H_{orthoNMe2}$); 3.37 (s, 6H, Ar-N(CH₃)₂); 2.92 (s, 12H, Ar-N(CH₃)₂). **¹SC NMR** (100 MHz, CDCl₃) δ 177.2 (C-Ar₃), 156.9 (C-NMe₂), 156.4 (C=NMe₂), 142.2 (C_{Ar}), 140.9 (C_{Ar}), 140.5 (C_{Ar}), 138.0 (C_{Ar}), 130.5 (C_{Ar}), 129.2 (C_{Ar}), 128.8 (C_{Ar}), 128.2 (C_{Ar}), 127.4 (C_{Ar}), 127.1 (C_{Ar}), 116.9 (C_{orthoCNMe2}), 113.2 (C_{orthoCNMe2}), 43.3 (ArN(CH₃)₂), 40.9 (Ar-N(CH₃)₂). **HRMS-ESI** (m/z): calculated for C₃₇H₃₈N₃ 524.3060 (M⁺), found 524.3068 (M⁺). **UV** (10 mM Tris-HCl, 0.1M NaCl, pH=7.06): λ _{max} 232 nm (ε 715875), 582 (76617).

4.1.6 Synthesis of 1f

2-phenyl-4-bromo-N,N-dimethylaniline (1 g, 3.63 mmol) was dissolved in THF (10 mL) and cooled to -78 °C. n-BuLi (1.65 mL, 2.3M in cyclohexane, 3.8 mmol) was added dropwise and the solution was stirred at -78 °C for 15 minutes. Then ethyl-3-phenyl-4-dimethylaminobenzoate (325 mg, 1.21 mmol) dissolved in THF (2 mL) was added dropwise at -78 °C. The solution was allowed to warm to room temperature and stir for 4 hours. A solution of 1M HCl (10 mL) was then added and the mixture was stirred for 30 minutes. Chloroform (20 mL) was added and the phases were separated. The aqueous phase was further extracted with chloroform (3x 10 mL); the combined organic extracts were once washed with 20 ml sat. aq. NaCl, dried over anhydrous Na₂SO₄, filtered, and concentrated under reduced pressure. Purification of the residue by size exclusion chromatography (Sephadex LH-20, chloroform) afforded 1f (503 mg, 0.78 mmol, 65%) as a blue solid, m.p. 80-83 °C (dec). ¹H NMR (400 MHz, CDCl₃) δ 7.51 (d, J= 7.3 Hz, 3H, Ar-H); 7.45-7.38 (m, 15H, Ar-H); 7.32 (d, J=2.3 Hz, 3H, Ar-H_{orthoPh}); 7.24 (d, J=9.0 Hz, 3H, Ar-H_{orthoNMe2}); 2.96 (s, 18 H, Ar-N(CH_3)₂). ¹³C NMR (100 MHz, CDCl₃) δ 176.8 (C-Ar₃), 157.3 (C-NMe₂)), 142.8 (C_{Ar}), 140.9 (C_{Ar}), 138.6 (C_{Ar}), 130.5 (C_{Ar}) , 129.0 (C_{Ar}) , 128.9 (C_{Ar}) , 128.2 (C_{Ar}) , 127.5 (C_{Ar}) , 117.3 (CorthoCNMe2), 43.5 (Ar-N(CH₃)₂). **HRMS-ESI** (m/z): calculated for $C_{43}H_{42}N_3$ 600.3373 (M⁺), found 600.3376 (M⁺). UV (10 mM Tris-HCl, 0.1M NaCl, pH=7.06): λ_{max} 260 nm (ϵ 136050), 320 (53177), 602 (42885).

4.1.7 Synthesis of 2a

1,2-diiodobenzene (330 mg, 1 mmol) and 2-(methoxycarbonyl)phenylboronic acid (396 mg, 2.2 mmol) were dissolved in a 4:1 toluene:water mixture (10 mL) and K₂CO₃ (607 mg, 4.4 mmol) and Pd(PPh₃)₄ (116 mg, 0.1 mmol, 10 mol%) were added. The mixture was heated to 95 °C under argon and stirred for 24 hours. After cooling to room temperature, water (10 mL) and ether (10 mL) were added, and the phases were separated. The aqueous phase was extracted twice with ether (2x10 mL) and the combined organic phases were dried over anhydrous sodium sulfate, filtered, and concentrated in vacuo. The crude oil was taken up in 2:1 hexanes: ethyl acetate and rapidly flushed through a plug of silica gel; concentration in vacuo furnished material sufficiently pure for the next step. 4-bromo-N,N-dimethylaniline (1 g, 5 mmol) was dissolved in THF (10 mL) and cooled to -78 °C. n-BuLi (2.17 mL, 2.3M in cyclohexane, 5 mmol) was added dropwise and the solution was stirred at -78 °C for 15 minutes. Then the diester intermediate from the previous step (~1 mmol) dissolved in THF (2 mL) was added dropwise at -78 °C. The solution was allowed to warm to room temperature and stir for four hours. A solution of 1 M HCl (10 mL) was then added, and the mixture was stirred for 30 minutes. Chloroform (20 mL) was added, and the phases were

separated. The aqueous phase was further extracted with chloroform (3 x 10 mL); the combined organic extracts were once washed with 20 ml sat. aq. NaCl, dried over anhydrous Na₂SO₄, filtered, and concentrated under reduced pressure. Purification by size exclusion chromatography (Sephadex LH-20, Chloroform) afforded 2a (340 mg, 0.43 mmol, 43%) as a dark green solid, m.p. 220-221 °C. ¹H NMR (400 MHz, CDCl₃) δ 7.40 (t, *J*=8.1 Hz, 2H, Ar-H); 7.28 (m, 4H, Ar-H); 7.10 (d, J=7.5 Hz, 2H, Ar-H); 7.01 (d, *J*=7.4 Hz, 2H, Ar-*H*); 6.88 (m, 7H, Ar-*H*); 6.77-6.71 (m, 7H, Ar-H); 6.57 (d, J=9.1 Hz, 4H, Ar-H_{orthoNMe2}); 3.46 (s, 10H, Ar- $N(CH_3)_2$); 3.21 (s, 14H, Ar-N(CH₃)₂). ¹³C NMR (100 MHz, CDCl₃) δ 175.8 (C-Ar₃), 156.9 (C=NMe₂), 155.7 (C-NMe₂), 144.7 (C_{Ar}) , 141.2 (C_{Ar}) , 138.8 (C_{Ar}) , 138.7 (C_{Ar}) , 137.8 (C_{Ar}) , 135.2 (C_{Ar}) , 132.6 (C_{Ar}) , 132.4 (C_{Ar}) , 132.3 (C_{Ar}) , 128.1 (C_{Ar}) , 127.8 (C_{Ar}), 127.6 (C_{Ar}), 126.8 (C_{Ar}), 114.6 (C_{orthoCNMe2}), 112.8 (CorthoCNMe2), 41.6 (Ar-N(CH₃)₂), 40.9 (Ar-N(CH₃)₂). HRMS-ESI (m/z): calculated for $C_{52}H_{52}N_4$ 366.2091 (M²⁺), found 366.2094 (M^{2+}) . UV (10 mM Tris-HCl, 0.1M NaCl, pH=7.06): λ_{max} 202 nm $(\epsilon 204505), 322 (56710), 438 (62422), 638 (209425).$

4.1.8 Synthesis of 2b

5,6-dibromo-1,3-benzodioxole (280 mg, 1 mmol) and 4-(methoxycarbonyl)phenylboronic acid (540 mg, 3.0 mmol) were dissolved in a 4:1 toluene:water mixture (10 mL) and K₂CO₃ (690 mg, 5.0 mmol) and Pd(PPh₃)₄ (174 mg, 0.15 mmol, 15 mol%) were added. The mixture was heated to 95 °C under argon and stirred for 48 hours. After cooling to room temperature, water (10 mL) and ether (10 mL) were added, and the phases were separated. The aqueous phase was extracted twice with ether (2x10 mL) and the combined organic phases were dried over anhydrous sodium sulfate, filtered, and concentrated in vacuo. The crude oil was taken up in 2:1 hexanes:ethyl acetate and rapidly flushed through a plug of silica gel; concentration in vacuo furnished material sufficiently pure for the next step. 4-bromo-N,N-dimethylaniline (1 g, 5 mmol) was dissolved in THF (10 mL) and cooled to -78 °C. n-BuLi (2.17 mL, 2.3M in cyclohexane, 5 mmol) was added dropwise and the solution was stirred at -78 °C for 15 minutes. Then the diester intermediate from the previous step (~1 mmol) dissolved in THF (2 mL) was added dropwise at -78 °C. The solution was allowed to warm to room temperature and stir for four hours. A solution of 1 M HCl (10 mL) was then added, and the mixture was stirred for 30 minutes. Chloroform (20 mL) was added, and the phases were separated. The aqueous phase was further extracted with chloroform (3x 10 mL); the combined organic extracts were once washed with 20 ml sat. aq. NaCl, dried over anhydrous Na₂SO₄, filtered, and concentrated under reduced pressure. Purification by size exclusion chromatography (Sephadex LH-20, chloroform) afforded 2b (521 mg, 0.63 mmol, 63%) as a dark green solid, m.p. 117-120 °C (dec). ¹H NMR (400 MHz, CDCl₃) δ 7.21 (m, 12H, Ar-H); 7.18 (m, 4H, Ar-H); 6.93 (s, 2H, Ar-H); 6.85 (m, 8H, Ar-H_{orthoNMe2}); 6.04 (s, 2H, O-CH₂-O); ¹³C **NMR** (100 MHz, CDCl₃) 3.31 (m, 24H, Ar-N(CH_3)₂). δ 176.5 (C-Ar₃), 156.8 (C-NMe₂), 148.2 (C_{Ar}), 146.3 (C_{Ar}), 140.6 (C_{Ar}) , 137.6 (C_{Ar}) , 134.7 (C_{Ar}) , 133.2 (C_{Ar}) , 130.3 (C_{Ar}) , 127.0 (C_{Ar}), 113.8 (C_{orthoCNMe2}), 110.5 (C_{orthoCNMe2}), 101.9 (O-CH₂-O), 41.2 (Ar-N(CH_3)₂). **HRMS-ESI** (m/z): calculated for $C_{53}H_{52}N_4O_2$ 388.2039 (M²⁺), found 388.2046 (M²⁺). UV (10 mM Tris-HCl, 0.1M NaCl, pH=7.06): λ_{max} 210 nm (ϵ 161235), 308 (71936), 440 (54252), 628 (214303).

4.1.9 Synthesis of 2c

5,6-diethynyl-1,3-benzodioxole³³ (170 mg, 1 mmol) and methyl-4-iodobenzoate (786 mg, 3 mmol) were dissolved in triethylamine (3 mL) and CuI (4 mg, 0.15 mmol) and Pd(PPh₃)₄ (116 mg, 0.1

mmol, 10 mol%) were added. The mixture was heated to 60 °C under argon for 24 hours. After cooling to room temperature, water (10 mL) and ether (10 mL) were added, and the phases were separated. The aqueous phase was extracted twice with ether (2x10 mL) and the combined organic phases were dried over anhydrous sodium sulfate, filtered, and concentrated in vacuo. The crude material was taken up in 2:1 hexanes:ethyl acetate and rapidly flushed through a plug of silica gel; concentration in vacuo furnished material sufficiently pure for the next step. 4-bromo-N,N-dimethylaniline (1 g, 5 mmol) was dissolved in THF (10 mL) and cooled to -78 °C. n-BuLi (2.17 mL, 2.3M in cyclohexane, 5 mmol) was added dropwise and the solution was stirred at -78 °C for 15 minutes. Then the diester intermediate from the previous step (~1 mmol) dissolved in THF (2 mL) was added dropwise at -78 °C. The solution was allowed to warm to room temperature and stir for four hours. A solution of 1 M HCl (10 mL) was then added, and the mixture was stirred for 30 minutes. Chloroform (20 mL) was added, and the phases were separated. The aqueous phase was further extracted with chloroform (3x 10 mL); the combined organic extracts were once washed with 20 ml sat. aq. NaCl, dried over anhydrous Na₂SO₄, filtered, and concentrated under reduced pressure. Purification by size exclusion chromatography (Sephadex LH-20, Chloroform) afforded 2c (478 mg, 0.53 mmol, 53%) as a dark green solid, m.p. 110-113 °C. ¹H NMR (400 MHz, CDCl₃) δ 7.67 (d, J=7.1 Hz, 4H, Ar-H); 7.32 (m, 13H, Ar-H); 6.95 (d, *J*=7.7 Hz, 9H, Ar-*H*_{orthoNMe2}); 6.06 (s, 2H, O-C*H*₂-O); 3.35 (m, 24H, Ar-N(CH_3)₂). ¹³C NMR (100 MHz, CDCl₃) δ 175.6 (C-Ar₃), 156.9 (C-NMe₂), 148.5 (C_{Ar}), 140.6 (C_{Ar}), 139.2 (C_{Ar}), 134.9 (C_{Ar}), 131.4 (C_{Ar}), 128.3 (C_{Ar}), 127.2 (C_{Ar}), 119.9 (C_{orthoCNMe2}), 114.1 $(C_{orthoCNMe2})$, 111.7 (C_{sp}) , 102.3 $(O-CH_2-O)$, 92.0 (C_{sp}) , 41.3 (Ar-C) $N(CH_3)_2$). **HRMS-ESI** (m/z): calculated for $C_{57}H_{52}N_4O_2$ 412.2040 (M²⁺), found 412.2037 (M²⁺). UV (10 mM Tris, 0.1M NaCl, pH=7.06): λ_{max} 204 nm (ϵ 317547), 266 (128225), 322 (121537), 462 (103221), 640 (214303).

4.1.10 Synthesis of **2d**

Methyl 4-[(diethoxyphosphinyl)methyl]benzoate² (429 mg, 1.5 mmol) was dissolved in THF (5 mL) and cooled to 0 °C. Then sodium hydride (60 mg, 1.5mmol, 60% dispersion in mineral oil) was added and the mixture was allowed to stir for 30 minutes. Then 1,3-benzodioxole-5,6-dicarboxyaldehyde (174.8 mg, 1 mmol) was added and the mixture was stirred overnight. Water (10 mL) and ether (10 mL) were added, and the phases were separated. The aqueous phase was extracted twice with ether (2x10 mL) and the combined organic phases were dried over anhydrous sodium sulfate, filtered, and concentrated in vacuo. The crude material was taken up in 3:1 hexanes:ethyl acetate and rapidly flushed through a plug of silica gel; concentration in vacuo furnished material sufficiently pure for the next step. 4-bromo-N,N-dimethylaniline (1 g, 5 mmol) was dissolved in THF (10 mL) and cooled to -78 °C. n-BuLi (2.17 mL, 2.3M in cyclohexane, 5 mmol) was added dropwise and the solution was stirred at -78 °C for 15 minutes. Then the diester intermediate from the previous step (~1 mmol) dissolved in THF (2 mL) was added dropwise at -78 °C. The solution was allowed to warm to room temperature and stir for four hours. A solution of 1 M HCl (10 mL) was then added, and the mixture was stirred for 30 minutes. Chloroform (20 mL) was added, and the phases were separated. The aqueous phase was further extracted with chloroform (3x 10 mL); the combined organic extracts were once washed with 20 ml sat. aq. NaCl, dried over anhydrous Na₂SO₄, filtered, and concentrated under reduced pressure. Purification by size exclusion chromatography (Sephadex LH-20, Chloroform) afforded 2d (360 mg, 0.4 mmol, 40%) as a dark green solid, m.p. 191-195 °C (dec). ¹H NMR (400 MHz, CDCl₃) δ 7.76 (m, 8H, Ar-H); 7.39 (m, 12H, Ar-H); 7.15 (s,

2H, Ar-H); 7.00 (d, J=9.2 Hz, 8H, Ar- $H_{orthoNMe2}$); 6.05 (s, 2H, O-C H_2 -O); 3.37 (s, 24H, Ar-N(C H_3)₂). ¹³C NMR (100 MHz, CDCl₃) δ 176.8 (C-Ar₃), 156.8 (C-NMe₂), 148.6 (C_{Ar}), 142.7 (C_{Ar}), 140.7 (C_{Ar}), 138.4 (C_{Ar}), 135.9 (C_{Ar}), 135.1 (C_{Ar}), 133.3 (C_{sp2}), 133.2 (C_{sp2}), 130.6 (C_{Ar}), 130.5 (C_{Ar}), 130.3(C_{Ar}), 129.5(C_{sp2}), 128.8 (C_{Ar}), 127.2 (C_{Ar}), 126.7 (C_{sp2}), 113.8 (C_{orthoCNMe2}), 106.1 (O-CH₂-O), 41.3 (Ar-N(CH₃)₂). **HRMS-ESI** (m/z): calculated for C₅₇H₅₆N₄O₂ 414.2196 (M²⁺), found 414.2184 (M²⁺). **UV** (0.1M Tris, 0.1M NaCl, pH=7.06): λ_{max} 204nm (ϵ 297848), 314 (110774), 628 (214303).

4.1.11 Synthesis of 2e

1,2-benzenedimethanol (138 mg, 1 mmol) and methyl-4hydroxybenzoate (334 mg, 2.2 mmol) were dissolved in THF (5 mL) and triphenylphosphine (577 mg, 2.2 mmol) was added. The solution was stirred temperature at room diisopropylazodicarboxylate (433 uL, 2.2 mmol) was added dropwise and the solution was stirred for 2 hours. Water (10 mL) and ether (10 mL) were added, and the phases were separated. The aqueous phase was extracted twice with ether (2x10 mL) and the combined organic phases were dried over anhydrous sodium sulfate, filtered, and concentrated in vacuo. The crude material was chromatographed over silica gel ($10:1 \rightarrow 4:1$ hexanes:ethyl acetate) to afford material the intermediate diester. 4-bromo-N,Ndimethylaniline (1 g, 5 mmol) was dissolved in THF (10 mL) and cooled to -78 °C. n-BuLi (2.17 mL, 2.3M in cyclohexane, 5 mmol) was added dropwise and the solution was stirred at -78 °C for 15 minutes. Then the diester intermediate from the previous step (~1 mmol) dissolved in THF (2 mL) was added dropwise at -78 °C. The solution was allowed to warm to room temperature and stir for four hours. A solution of 1 M HCl (10 mL) was then added, and the mixture was stirred for 30 minutes. Chloroform (20 mL) was added, and the phases were separated. The aqueous phase was further extracted with chloroform (3x 10 mL); the combined organic extracts were once washed with 20 ml sat. aq. NaCl, dried over anhydrous Na₂SO₄, filtered, and concentrated under reduced pressure. Purification by size exclusion chromatography (Spehadex LH-20, chloroform) afforded 2e (529 mg, 0.61 mmol, 61%) as a dark green solid, m.p. 242-245°C. ¹H NMR (400 MHz, CDCl₃) δ 7.49 (m, 2H, Ar-H); 7.35 (m, 3H, Ar-H); 7.33-7.29 (m, 12H, Ar-H); 7.13 (d, J=8.9 Hz, 4H, Ar-H_{orthoO}); 6.83 (d, J=9.3 Hz, 8H, Ar-H_{orthoNMe2}); 5.32 (s, 4H, ArCH₂O); 3.23 (s, 24H, Ar- $N(CH_3)_2)$). ¹³C NMR (100 MHz, CDCl₃) δ 177.6 (C-Ar₃), 163.6 $(C\text{-OCH}_2)$, 156.6 $(C\text{-NMe}_2)$, 140.6 (C_{Ar}) , 137.7 (C_{Ar}) , 134.2 (C_{Ar}) , 131.9 (C_{Ar}) , 129.2 (C_{Ar}) , 128.8 (C_{Ar}) , 126.8 (C_{Ar}) , 115.3 (CorthoCNMe2), 113.3 (CorthoCNMe2), 68.6 (ArCH2O), 40.9 (Ar- $N(CH_3)_2$). **HRMS-ESI** (m/z): calculated for $C_{54}H_{56}N_4O_2$ 396.2196 (M²⁺), found 396.2215 (M²⁺). UV (10 mM Tris, 0.1M NaCl, pH=7.06): λ_{max} 204 nm (ϵ 114333), 296 (29027), 448 (62834), 570 (174000).

4.2 Competitive ethidium bromide displacement

Constant concentrations of CT-DNA (1.0 μ M/bp) and EtBr (0.5 μ M) in the presence or absence of netropsin (0.5 μ M) or methyl green (0.5 μ M) were titrated with increasing concentrations of the ligands **1a-1f** and **2a-2e** (from 100 μ M and 10 μ M stock solutions) in buffer (10 mM Tris-HCl, pH=7.0). The maximum emission wavelength was 590 nm when the excitation wavelength was 520 nm. Fluorescence titrations were recorded from 520 nm to 692 nm after an equilibration period of 3 min. Ex Slit (nm) = 10.0; Em Slit (nm) = 10.0; Scan Speed (nm/min) = 200. K_{app} =9.5x10⁶ M⁻¹ x C_{ethidium}/C₅₀.

UV thermal denaturation samples (2 mL) were prepared by mixing CT-DNA in 10 mM Tris-HCl buffer (pH 7.0) in 1 cm path length quartz cuvettes. The DNA to ligand ratio was 30:1. Absorbance readings were taken for temperature ranging from 25 °C to 95 °C. Temperature was increased gradually with a speed of 1°C/min with an absorbance reading every 2°C. First derivative plots were used to determine the T_M value.

4.4 Solution Viscosity studies

Viscosity experiments were performed with an Ostwald viscometer in a constant water bath at $23.0 \pm 1^{\circ} C.$ Solutions of constant DNA concentrations (300 $\mu\text{M/bp})$ and varying ligand concentrations in 10 mM Tris-HCl buffer (pH 7.0) were incubated for 30 minutes. A digital stopwatch was used to record the flow time. The relative viscosity was calculated as from the following equation:

$\eta = t - t_o / t_o$

Where t_o and t are the flow time in the absence and presence of the ligand. η is the viscosity in the presence of the ligand and η_o is the viscosity in the absence of ligand. The data were graphed as $(\eta/\eta_o)^{1/3}$ vs. [ligand]/[DNA].

4.5 Circular dichroism and UV studies

Small aliquots (0.6-5.0 $\mu L)$ of concentrated ligands 1a-1f and 2a-2e (1 mM) were added to a solution (2 mL, 10 mM tris-HCl, pH 5.0) of CT-DNA (80 $\mu M/bp)$ or DDD hairpin (8.8 $\mu M)$, inverted twice, and incubated for 5 min at 20 °C. The CD spectra were then recorded as an average of three scans from 215 to 350 nm and data recorded in 0.5 nm increments. UV spectra were collected under identical conditions over the same wavelength range.

4.6 Isothermal titration calorimetry studies

ITC thermograms were recorded for titrations performed at 30 °C (except for compound **2e** performed at 27 °C with 50 injections, 5 mL each, 5s duration) under the following conditions: DP=6, 307 rpm, 10 mL injections, 10s duration with 120s, 2s filter, initial delay of 120s, total of 25 injections (Microcal VP-ITC). The initial conditions for the titrations involved 100 μ M ligand in the syringe and 100 μ M/bp CT DNA or 10 μ M hairpins in the cell, common buffer 10 mM Tris-HCl, pH=7.0. Prior to data analysis in Origin software, subtraction of buffer to CT DNA titrations under identical conditions was performed to account for heats of dilution. A single-site binding model was applied to obtain vales of K, N, ΔH , ΔS for each experiment.

4.7 Agarose gel electrophoresis studies

Plasmid pUC-19 was linearized with AlwNI at 37 °C for 30 minutes and then incubated with varying concentrations of **1a-1f** and **2a-2e**. BamHI was then added and digestion proceeded for 30 minutes at 37 °C. Samples were then loaded onto a 1% agarose gel containing 0.5 μ g/L ethidium bromide and run at 120V for 40 minutes. A UV transilluminator was used to visualize the gel.

Compounds 1a, 1b, 2d, and 2e were minimized in Spartan 14 for Macintosh (Wavefunction, Inc., Irvine, CA). Molecular docking studies were performed with 1a, 1b, and 2e and the Dickerson Drew dodecamer (5'CGCGAATTCGCG-3') (PDB 436D), and with 2d and the NFAT sequence (10WR) using Autodock vina. The search space included both major and minor

4.9 Electrostatic potential and LUMO maps

Utilizing Spartan 20 for Macintosh (Wavefunction, Inc. Irvine, CA) compound **2d** and the base pairs of 5-GC-3' were energy minimized (density functional, wB97X-D, 6-31G*) and electrostatic potential maps and HOMO/LUMO maps were generated.

Acknowledgments

This paper is dedicated to the memory of Professor Yoshito Kishi. We thank the National Science Foundation (CHE-2003261) and the donors of the American Chemical Society Petroleum Research fund (62233-UR1) for their generous support of our research program. DC thanks the NIH RISE program (GM008395) for support.

References and notes

- (a) J. M. Gottesfeld, J. M., L. Neely, J. W. Trauger, E. E. Baird, and P. B. Dervan, *Nature* 1997, **387**, 202. (b) C.-H. Leung, D. S.-H. Chan, V. P-Y. Ma, and D.-L. Ma, *Med. Res. Rev.* 2013, **33**, 823. (c) T. Berg, *Curr. Opin. Chem. Biol.* 2008, **12**, 464.
- 2 (a) P. I. Hamilton and D. P. Arya, *Nat. Prod. Rep.* 2012, 29, 134. (b) W. C. Tse and D. L. Boger, *Chem. Biol.* 2004, 11, 1607
- 3 (a) L. D. Williams and Q. Gao, *Biochemistry* 1992, 31, 4315. (b) M. E. Peek, L. A. Lipscomb, J. A. Bertrand, Q. Gao, B. P. Roques, C. Garbay-Jaureguiberry, and L. D. Williams, *Biochemistry* 1994, 33, 3794. (c) M. E. Peek, L. A. Lipscomb, J. Haseltine, Q. Gao, B. P. Roques, C. Garbay-Jaureguiberry, and L. D. Williams, *Bioorg. Med. Chem.* 1995, 3, 693.
- 4 (a) C. L. Mazzitelli, Y. Chu, J. J. Reczek, B. L. Iverson, and J. S. Brodbelt, J. A. Soc. Mass Spectrom. 2007, 18, 311. (b) V. Guelev, J. Lee, J. Ward, S. Sorey, D. W. Hoffman, and B. L. Iverson, Chem. Biol. 2001, 8, 415.
- 5 (a) S. Kumar, L. Xue, and D. P. Arya, *J. Am. Chem. Soc.* 2011, **133**, 7361. (b) B* form DNA refers to AT rich DNA sequences that contain long A tracts leading to an unusually narrow minor groove: N. V. Hud and J. Plavec, *Biopolymers* 2003, **69**, 144.
- 6 D. V. Bernikova, N. I. Sosnin, O. A. Federova, and H. Ihmels, *Org. Biomol. Chem.* 2018, **16**, 545.
- 7 (a) A. Stefanocci, J. Amato, D. Brancaccio, B. Pagano, A. Randazzo, F. Santoro, L. Mayol, S. Learte-Aymami, J. Rodriguez, J. L. Mascarenas, E. Novellino, A. Carotenuto, and A. Mollica, *Bioog. Chem.* 2021, 112, 104836. (b) A. Stefanucci, J. Mosquera, E. Vazquez, J. L. Mascarenas, E. Novellino, and A. Mollica, A. ACS Med. Chem. Lett. 2015, 6 1220
- 8 (a) W. Muller and F. Gautier, Eur. J. Biochem. 1975, 54, 385. (b) L. P. G. Wakelin, A. Adams, C. Hunter, and M. J. Waring, Biochemistry 1981, 20, 5779. (c) Y. Chen, J. Wang, Y. Zhang, L. Xi, T. Gao, B. Wang, and R. Pei, Photochem. Photobiol. Sci. 2018, 17, 800. (d) S. K. Kim and B. Norden, FEBS Lett. 1993, 315, 61.

- 9 O. Nunez, O.; B. Chavez, R. Shaktah, P. Pereda Garcia, and T. Minehan, *Bioorg. Chem.* 2019, **83**, 297.
- 10 D. F. Taber, R. P. Meagley, and D. J. Supplee, *J. Chem. Ed.* 1996, **73**, 259.
- 11 C. C. Barker, M. H. Bride, and A. Stamp, *J. Chem. Soc.* 1959, 3957.
- 12 (a) A. R. Morgan, J. S. Lee, D. E. Pulleybank, N. L. Murray, and D. H. Evans, *Nucleic Acids Res.* 1979, **7**, 547. (b) We observed that the fluorescence emission intensity of the CV derivatives above 600 nm (excitation wavelength ~ 550 nm) is minimally altered in the presence of CT DNA; furthermore, the quantum yield of CV in the absence of DNA is 0.019, which is approximately 10-fold lower than that of ethidium bromide (0.15). As a result, ethidium bromide was chosen as the fluorescent reporter for our competition experiments. See: L. A. Brey, G. B. Schuster, H. G. Druckamer, *J. Chem. Phys.* 1977, **67**, 2648.
- 13 M. Sirajuddin, S. Ali, and A. Badshah, J. PhotoChem. Photobiol. B: Biology 2013, 124, 1.
- 14 (a) D. Suh and J. B. Chaires *Bioorg. Med. Chem.* 1995, 3,723. (b) P. C. Dedon, *Curr. Protoc. Nucleic Acid. Chem.* John Wiley and Sons, New York, 2000, 8.1.1.
- 15 (a) E. W. White, F. Tanious, M. A. Ismail, A. P. Reska, S. Neidle, D. W. Boykin, and W. D. Wilson *Biophys. Chem.* 2007, **126**, 140. (b) K. Triantafillidi, K. Karidi, J. Malina, and A. Garoufis, *Dalton Trans.* 2009, 6403. (c) M. J. Hannon, V. Moreno, M. J. Prieto, E. Moldrheim, E. Sletten, I. Meistermann, C. J. Isaac, K. J. Sanders, and A. Rodger, *Angew. Chem., Int. Ed.* 2001, **40**, 880.
- 16 (a) N. C. Garbett, P. A. Ragazzon, and J. B Chaires, *Nature Protoc.* 2007, 2, 3166. (b) Monitoring the titration of CT DNA with compound 2b by CD spectroscopy also provided evidence of minor groove binding (see supporting information), although the competitive inhibition assays indicate lowest affinities for CT DNA in the presence of methyl green.
- 17 (a) E. A. Lewis, M. Munde, S. Wang, M. Rettig, V. Le, V. Machha, and W. D. Wilson, *Nucleic Acids Res.* 2011, 11, 1.
 (b) N. J. Buurma and I. Haq, *Methods* 2007, 42, 162. (c) D. S. Pilch, N. Poklar, E. E. Baird, and P. Dervan, *Biochemistry* 1999, 38, 2143. (d) D. Retzeperis, T. J. Dwyer, B. H. Geierstanger, J. G. Pelton, D. E. Wemmer, and L. A. Marky *Biochemistry* 1995, 34, 2937. (e) ITC titrations of CT DNA with compound 2b revealed roughly equivalent enthalpic (ΔH=-3.91±0.08 kcal/mol) and entropic (-TΔS=-4.3 kcal/mol) contributions to the binding free energy.
- 18 (a) J. B. Chaires, Arch. Bioch. Biophys. 2006, 453, 26. (b)J. B. Chaires Biopolymers 1997, 44, 201.
- 19 (a) C. M. Lukacs, R. Kucera, I. Schildkraut, and A. K. Aggarawal, *Nature Struct. Biol.* 2000, **2**, 134. (b) A. K. Aggarwal *Curr. Opin. Struct. Biol.* 1995, **5**, 11. (c) M. Deibert, S. Grazulis, A. Janulaitis, V. Siksnys, and R. Huber, *EMBO J.* 1999, **18**, 5805.
- 20 S. M. Forrow, M. Lee, R. L. Souhami, and J. A. Hartley Chem. Biol. Interact. 1995, 96, 125.

- 21 (a) W. C. Tse and D. L. Boger, Acc. Chem Res. 2004, 37,
 61. (b) D. L. Boger, W. C. Tse, Bioorg. Med. Chem. 2001,
 9, 2511.
- 22 J. C. Stroud and L. Chen, J. Mol. Biol. 2003, 334, 1009.
- 23 J. Li, J. P. Rodriguez, F. Niu, M. Pu, J. Wang, L. W. Hung, Q. Shao, Y. Zhu, W. Ding, Y. Liu, Y. Da, Z. Yao, J. Yang, Y. Zhao, G. H. Wei, G. Cheng, Z. J. Liu, S. Ouyang, *Proc. Natl. Acad. Sci. USA* 2016, 113, 13015.
- 24 S. K. Nair and S. K. Burley, Cell 2002, 112, 193.
- 25 V. Tereshko, G. Minasov, and M. Egli, J. Am. Chem. Soc. 1999, 121, 470.
- 26 (a) O. Trott and A. J. Olson, J. Comput. Chem. 2010, 31, 455. (b) The search space included both major and minor grooves as well as the phosphate backbone of DNA. The ligand was first minimized using Spartan 20 for Macintosh (Wavefunction, Inc., Irvine, CA).
- 27 R. W. Newberry and R. T. Raines Acc. Chem. Res. 2017, 50, 1838.
- (a) S. Wang, P. W. Huber, M. Cui, A. W. Czarnik, and H. Y. Mei, Biochemistry 1998, 37, 5549.
 (b) B. Francois, R. J. Russell, J. B. Murray, F. Aboul-ela, B. Masquida, Q. Vicens, and E. Westhof, Nucleic Acids Res. 2005, 33, 5677.
 (c) S. H. Verhelst, P. J. Michiels, G. A. van der Marel, C. A. van Boeckel, and J. H. van Boom, ChemBioChem 2004, 5, 937.
 (d) M. Kaul, C. M. Barbieri, and D. S. Pilch, J. Mol. Biol. 2005, 346, 119.
 (e) V. K. Misra and B. Honig, Proc. Natl. Acad. Sci. USA 1995, 92, 4691.
- 29 W.D. Wilson, F. A. Tanious, M. Fernandez-Saiz, C. T. Rigl, Methods Mol. Biol. Drug-DNA Interact. Protoc. 1997, 90, 219.
- 30 (a) L. Kittler, A. Bell, B. C. Baguley, and G. Lober, Biochem. Mol. Biol. Internat. 1996, 40, 263. (b) S. M. Forrow, M. Lee, R. L. Souhami, and J. A. Hartley Chemico-Biol. Interact. 1995, 96, 125.
- 31 Electrostatic potential maps for **4b** and the base pairs of 5'-GA-3' (energy minimized: density functional, wB97X-D, 6-31G*) were generated by Spartan 20 for Macintosh (Wavefunction Inc, Irvine, CA).
- 32 K. E. Reinert, J. Biomol. Struct. Dyn. 1991, 9, 331.
- 33 M. Urbani and T. Torres, Chem. Eur. J. 2020, 26, 1683.
- 34 B.D. Wall, Y. Zhou, S. Mei, H. A. K. Ardona, A. L. Ferguson, and J. D. Tovar, *Langmuir* 2014, **30**, 11375.

Supplementary Material

Supplementary data (synthetic procedures, spectroscopic data and ¹H and ¹³C NMR spectra, DNA binding studies) associated with this article can be found, in the online version, at.